Structural Monitoring and Maintenance, *Vol. 5, No. 2 (2018) 231-242*
DOI: https:// doi.org/10.12989/smm.2018.5.2.231

Damage detection of subway tunnel lining through statistical pattern recognition

Hong Yu[a], Hong P. Zhu[b], Shun Weng[*], Fei Gao[c], Hui Luo[d] and De M. Ai[e]

School of Civil Engineering and Mechanics, Huazhong University of Science and Technology, Wuhan 430074, China

(Received January 31, 2018, Revised March 26, 2018, Accepted March 28, 2018)

Abstract. Subway tunnel structure has been rapidly developed in many cities for its strong transport capacity. The model-based damage detection of subway tunnel structure is usually difficult due to the complex modeling of soil-structure interaction, the indetermination of boundary and so on. This paper proposes a new data-based method for the damage detection of subway tunnel structure. The root mean square acceleration and cross correlation function are used to derive a statistical pattern recognition algorithm for damage detection. A damage sensitive feature is proposed based on the root mean square deviations of the cross correlation functions. X-bar control charts are utilized to monitor the variation of the damage sensitive features before and after damage. The proposed algorithm is validated by the experiment of a full-scale two-rings subway tunnel lining, and damages are simulated by loosening the connection bolts of the rings. The results verify that root mean square deviation is sensitive to bolt loosening in the tunnel lining and X-bar control charts are feasible to be used in damage detection. The proposed data-based damage detection method is applicable to the online structural health monitoring system of subway tunnel lining.

Keywords: statistical pattern recognition; root mean square; cross correlation function; subway tunnel structure

1. Introduction

As ground transportation is congested in many cities, subway system has become increasingly important to urban people's daily commuting. The subway tunnel structures suffer attacks from mechanical, physical, and even chemical actions (Richards 2002). As a result, the subway tunnel structures deteriorate gradually during their service life. Structural health monitoring is concerned with the implementation of a damage detection strategy, which provides information about structure's conditions that help us to have a better understanding of the structural status (Yi *et al*. 2010, 2013, Farrar and Worden 2013, Chen and Xia 2017, Chen *et al*. 2017). Structural health

∗Corresponding author, Associate Professor, E-mail: wengshun@hust.edu.cn
[a] Ph.D. Student, E-mail: yuhong2016@hust.edu.cn
[b] Professor, E-mail: hpzhu@hust.edu.cn
[c] Professor, E-mail: hustgaofei@hust.edu.cn
[d] Professor, E-mail: luohui66@hust.edu.cn
[e] Ph.D., E-mail: aidemi12@hust.edu.cn

http://www.techno-press.org/?journal=smm&subpage=7 ISSN: 2288-6605 (Print), 2288-6613 (Online)

monitoring system is progressively seen as a cost effective way to minimize the risks of subway tunnel structures (Bennett *et al*. 2010). Feng *et al*. (2015) applied transmissibility function and cross correlation analysis to detect damages in subway tunnel structure. Zhou *et al*. (2012) developed a Timoshenko beam-Transfer Matrix Method to determine the relationship between the tunnel Young's modulus and the coupled resonance frequency.

The damage detection algorithms can be classified into two categories: model based algorithms and non-model based algorithms. Model based algorithms are essentially a kind of model updating procedure in which the structural physical parameters (stiffness, mass, and damping) are calibrated and updated using measured data (Xiao *et al*. 2015, Li *et al*. 2015). The main difficulties of these algorithms are that the updated physical parameters may be discrepant from the actual damage cases and these algorithms are usually sensitive to measurement noise (Noman *et al*. 2013). Non-model based algorithms do not require a physical model of the structure, so they provide an attractive alternative to model based algorithms. The definition of damage implies a comparison between two different states of the structure. Therefore, statistical pattern recognition techniques, implemented by means of machine learning algorithms, are very suitable for developing non-model based damage detection. The structural health monitoring process that cast within the statistical pattern recognition framework can be deployed into three portions: data acquisition and cleansing, feature selection and data compression, and statistical model development (Farrar *et al*. 2001). In particular, this paper will focus on feature selection and statistical model development portions.

The structural health monitoring process that cast within statistical pattern recognition framework do not require a physical model of structure, which makes it unfeasible to assess the structural health condition using the response time histories directly. For this reason, damage sensitive features need to be extracted from the acquired response time histories. The basic requirements of damage sensitive feature are its sensitivity to damage and its insensitivity to measurement noise. In order to perform statistical analysis, enough damage sensitive feature samples are required, and the damage sensitive feature extraction process will thus be repeated many times. In addition, the computational cost of damage sensitive feature should be small. Moreover, the damage sensitive feature extraction process should be as simple as possible to guarantee consistency of the damage detection results, irrespective of the user expertise level (Balsamo *et al*. 2014). In the field of statistical pattern recognition, time series analysis models have been widely utilized to extract damage sensitive features. Sohn *et al*. (2000) used auto-regressive model coefficients as damage sensitive features to discriminate the undamaged and damaged condition of a bridge column. The auto-regressive model coefficients are proved to be function of structural modal parameters (natural frequency, mode shape, and modal damping) by Pandit and Wu (1983). Sohn and Farrar (2001) used the standard deviation of the residual errors, which is derived from a combination of the auto-regressive and auto-regressive with exogenous inputs model, as damage sensitive features to locate damage. The premise of this approach is that the residual error increase when the structure experiences damage, especially when the modeling data is measured near the actual damage regions. Carden and Brownjohn (2008) used autoregressive moving average model coefficients to feed a statistical classifier, and the classifier is capable of forming new classes when the structure experiences damage. Mosavi *et al*. (2012) fitted the structural response time histories to the multivariate vector autoregressive models, and Mahalanobis distances of the coefficients are served as damage sensitive features.

Root mean square acceleration is a good indicator of the overall structural condition, so it is widely used in gait analysis research (Sekine *et al*. 2013) and gearbox condition evaluation

(Rzeszucinski *et al*. 2012). The cross correlation function between two response time histories measured on a structure excited by ambient excitation was shown to have the similar form of the system's impulse response function. The cross correlation function was used to assess the resonant frequencies and modal damping of structures (Farrar and Iii 1997). Zhu *et al*. (2010) defined a damage indicator by comparing the peak amplitude of the cross correlation function of the damaged structure versus the undamaged structure to identify and locate damage in a portal frame structure. The root mean square deviation is frequently used to measure the differences between datasets, and is more robust compared with other damage indices, such as cross correlation, mean absolute percentage deviation and relative deviation (Zhu *et al*. 2016).

In this study, the root mean square values of acceleration responses measured at two different points are used for cross correlation analysis, and cross correlation functions of the root mean square values are derived. Then, the root mean square deviation of normalized cross correlation functions before and after damage are chosen as damage sensitive features. Finally, statistical process control charts are utilized to monitor the variation of root mean square deviation before and after damage. Effectiveness of the algorithm is validated by the experimental study of a full-scale two-rings subway tunnel lining.

2. Root mean square acceleration for damage identification

Structural acceleration responses are widely used in structural damage detection as they contain information about structure's inherent dynamic properties. The acceleration time histories measured under the undamaged condition are divided into two datasets. One of those time histories is taken as the reference dataset, and the others are taken as the healthy dataset. The reference dataset is used as a reference condition of the tested structure and the healthy dataset is used for later damage sensitive feature extraction for healthy condition of the tested structure. Similarly, the acceleration time histories measured under each damaged condition are used to form the corresponding damage dataset. The damage dataset of each damaged condition is used to extract damage sensitive features for corresponding damage condition of the tested structure.

Suppose $x(t)$ is the acceleration time histories measured from the tested structure, a time window is adopted to divide $x(t)$ into N smaller data blocks, and each data block includes L data points (i.e., the length of $x(t)$ is $N \times L$). The root mean square value of each data block is calculated as (Vecer *et al*. 2005)

$$x_i^{rms} = \sqrt{\frac{1}{L}\sum_{j=1}^{L} x_{ij}^2} \tag{1}$$

where x_{ij} is the j-th (j = 1,2,…,L) member of i-th (i = 1,2,…,N) data block, and x_i^{rms} is the root mean square value of i-th data block. The root mean square acceleration of $x(t)$ can be gained by gathering the root mean square values of all data blocks

$$X^{rms} = [x_1^{rms}, x_2^{rms}, \cdots, x_i^{rms}, \cdots, x_N^{rms}] \tag{2}$$

From the definition of root mean square acceleration, it is obvious that it is irrelevant to the isolated peaks in the signal and is a significant descriptor of the overall condition of the tested structure.

3. Cross correlation function between two time serie

Suppose $x_p(t)$ and $x_q(t)$ are respectively the acceleration response time histories of measured points p and q, X_p^{rms} and X_q^{rms} are the root mean square acceleration of $x_p(t)$ and $x_q(t)$, respectively. Damage-induced changes in the physical properties will cause the inherent dynamic property changes of the structure. The relationship between X_p^{rms} and X_q^{rms} are determined by the inherent dynamic properties of the structure. Therefore, damage can be detected by comparing the relationship between X_p^{rms} and X_q^{rms} before and after damage.

The basic problem of cross correlation function is the description and modeling of the relationship between two time series. So, damage can be detected by comparing the cross correlation function between X_p^{rms} and X_q^{rms} before and after damage. In the relationship between two time series X_p^{rms} and X_q^{rms}, the series X_p^{rms} may be related to past lags of the series X_q^{rms}. The time-discretized cross correlation function between X_p^{rms} and X_q^{rms} is defined as (Feng *et al*. 2015)

$$R_{pq}(k)=\begin{cases}\dfrac{1}{N-k}\displaystyle\sum_{h=0}^{N-k-1}X_p^{rms}(h+k)X_q^{rms}(h), & 0\le k\le N-1\\ R_{qp}(-k), & -N+1\le k<0\end{cases} \tag{3}$$

where k is the time lags between X_p^{rms} and X_q^{rms}. The deterministic cross correlation function can be normalized by

$$\tilde{R}_{pq}(k)=\frac{R_{pq}(k)}{\sqrt{R_{pp}(0)}\sqrt{R_{qq}(0)}},\quad -N+1\le k\le N-1 \tag{4}$$

Cross correlation function is helpful for identifying lags of X_p^{rms} that might be useful predictors of X_q^{rms}. A positive value for k is a correlation between X_p^{rms} at a time after t and X_q^{rms} at time t, and a negative value for k is a correlation between X_p^{rms} at a time before t and X_q^{rms} at time t. For instance, considering k = +2, the cross correlation function value gives the correlation between $X_p^{rms}(t+2)$ and X_q^{rms}; considering k = −2, the cross correlation function value gives the correlation between $X_p^{rms}(t-2)$ and X_q^{rms}.

4. Root mean square deviation of cross correlation function

In this work, the root mean square deviation (RMSD) is utilized to estimate the amount of variations between the cross correlation functions before and after damage. It is denoted as the cross-correlation damage indicator RMSD^{pq}

$$\mathrm{RMSD}^{pq}=\sqrt{\frac{\sum_{k=-N+1}^{N-1}\left(\tilde{R}_{pq}^{D}(k)-\tilde{R}_{pq}^{R}(k)\right)^2}{\sum_{k=-N+1}^{N-1}\left(\tilde{R}_{pq}^{R}(k)\right)^2}}\times 100\% \tag{5}$$

where $\tilde{R}_{pq}^{R}(k)$ represents the normalized cross correlation function that derived from the

reference dataset; and $\tilde{R}_{pq}^{D}(k)$ represents the normalized cross correlation function that derived from the healthy dataset or the damage dataset. The superscripts *R* in $\tilde{R}_{pq}^{R}(k)$ represent 'reference', and the superscripts *D* in $\tilde{R}_{pq}^{D}(k)$ represent 'damage'.

5. Statistical modeling

X-bar control chart is the most commonly used statistical modeling technique and is very suitable for online structural health monitoring. In the field of quality control, X-bar control chart is widely used to monitor the changes of the selected features and to identify samples that are inconsistent with the past data sets (Sohn *et al*. 2000). Here X-bar control chart is utilized to detect the occurrence of damage. The RMSD^{pq} values extracted from the healthy dataset are used to construct the control limits. Suppose there are *n* sets of time histories in the healthy dataset, thus *n* corresponding RMSD^{pq} samples will be extracted. X-bar control chart is constructed by drawing a centerline (CL) at the sample mean and two additional horizontal lines corresponding to the upper and lower control limits (UCL and LCL) versus sample numbers. The centerline and two control limits are defined as

$$UCL, LCL = CL \pm Z_{\alpha/2}\frac{S}{\sqrt{n}}; CL = mean(\text{RMSD}_i^{pq}) \tag{6}$$

where the calculation of mean is with respect to all RMSD^{pq} samples extracted from the healthy dataset ($i = 1, \ldots, n$); $Z_{\alpha/2}$ is the percentage point of the normal distribution with zero mean and unit variance such that $P[Z \geq Z_{\alpha/2}] = \alpha/2$ (the probability of $Z \geq Z_{\alpha/2}$ is $\alpha/2$); S is the standard deviation of all the RMSD^{pq} samples that extracted from the healthy dataset.

The monitoring of damage occurrence is performed by plotting the RMSD^{pq} samples that extracted from the damage dataset along with the previously constructed control limits. If the system experienced damage, this would be likely to be indicated by an unusual number of samples outside the control limits. In this paper, a charted value outside the control limits is referred to as an outlier.

6. Experimental validation

The subject of the experiment is the full-scale two-rings subway tunnel lining shown in Fig. 1(a). It is located in the Hubei Key Laboratory of Control Structures at Huazhong University of Science & Technology. As shown in Fig. 1(b), the outside diameter of the tunnel lining is 4000 mm, the inside diameter is 3500 mm, and the width of each ring is 1200 mm. One full ring consists of 6 segments, including a top segment (F segment), two contiguous segments (L1 and L2 segments), and three standard segments (B1, B2 and B3 segments). The corresponding central angle of segment F is 29.0°, with L1, L2 53.0° and B1, B2, B3 75.0°. Twelve high strength bolts are used to connect the segments in radial direction and fourteen high strength bolts are used to connect the two rings in longitudinal direction. The tunnel lining is placed on the ground, and there is no constraint between the tunnel lining and ground.

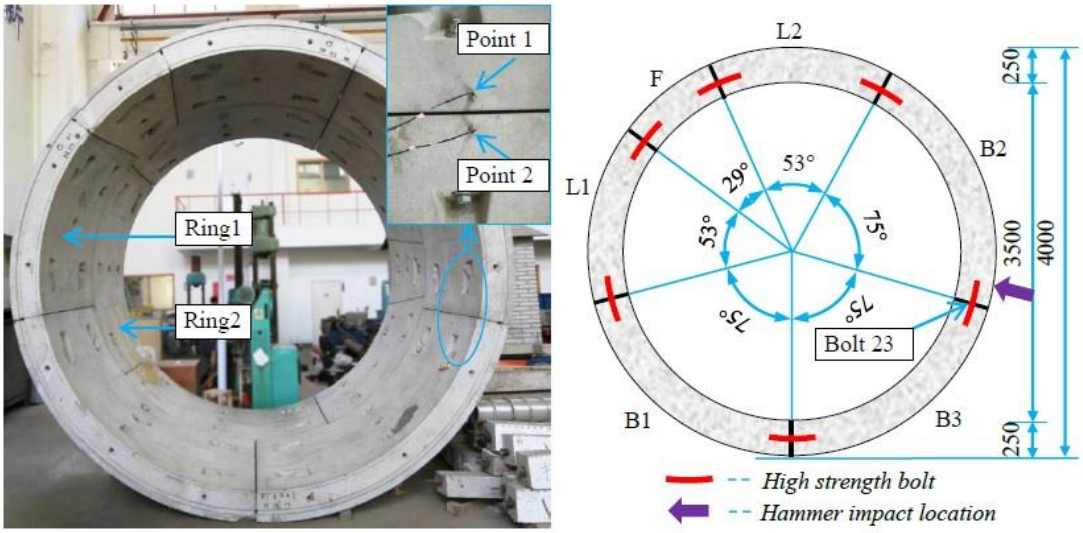

(a) Test site photo (b) Cross section of the Ring 1 (unit: mm)

Fig. 1 Full-scale tunnel lining

Table 1 Description of test cases

Case	Condition	Configuration
1	Undamaged(U)	Bolt 23 was not loosened
2	Damaged(D1)	Bolt 23 was loosened 180°
3	Damaged(D2)	Bolt 23 was loosened 270°
4	Damaged(D3)	Bolt 23 was removed

A series of tests were conducted on the tunnel lining with various damage conditions. In the tests, damage is simulated by loosening Bolt 23 (see Fig. 1(b)) that connect B2 segment and B3 segment. The four test cases are described in Table 1. Note that Cases 2 through 4 are considered as damage conditions when Case 1 is viewed as the undamaged condition.

Vibration testing was carried out on the tunnel lining in all the undamaged and damaged conditions. The tunnel lining was excited by a hammer with a hammerhead weighted about 1.5 kg. The hammer impact location was on the outside surface of the Ring 1, as denoted in Fig. 1(b). The hammer impact was in the direction that perpendicular to the surface of the lining.

Two DH187E accelerometers with the sensitivity of 50 mV/g were placed at measurement points 1 and 2, respectively (see Fig. 1(a)). The acceleration responses of B2 segment and B3 segment that perpendicular to the surface of the lining were measured. A 16-channel DH5922 acquisition system was used to record the structural responses. Antialiasing filters were used in the tests, and the data was sampled at 1000 Hz. Typical hit acceleration time histories of measurement points 1 and 2 are shown in Fig. 2. The measured structural responses attenuated to a neglectable value within a very short time. The frequency responses of measurement points 1 and 2 under four

conditions are plotted in Fig. 3. Compared with the undamaged condition U, the maximum resonance peaks of damaged condition D1, D2 and D3 in the frequency responses shift to lower frequencies. Maybe it is because the loosening of Bolt 23 reduces the global stiffness of the tunnel lining, thus bring the reduction of natural frequencies.

The tunnel lining was impacted 21 times in the undamaged condition and 20 times in each damaged condition to eliminate measurement error. Thus there were 21 sets of acceleration response time histories recorded in the undamaged condition and 20 sets of acceleration response time histories recorded in each damaged condition. One set of those time histories recorded in the undamaged condition is taken as the reference dataset, and the other 20 sets of time histories recorded in the undamaged condition are taken as the healthy dataset (i.e., n = 20 in Eq. (6)). The 20 sets of time histories recorded in each damaged condition are taken as the corresponding damage dataset.

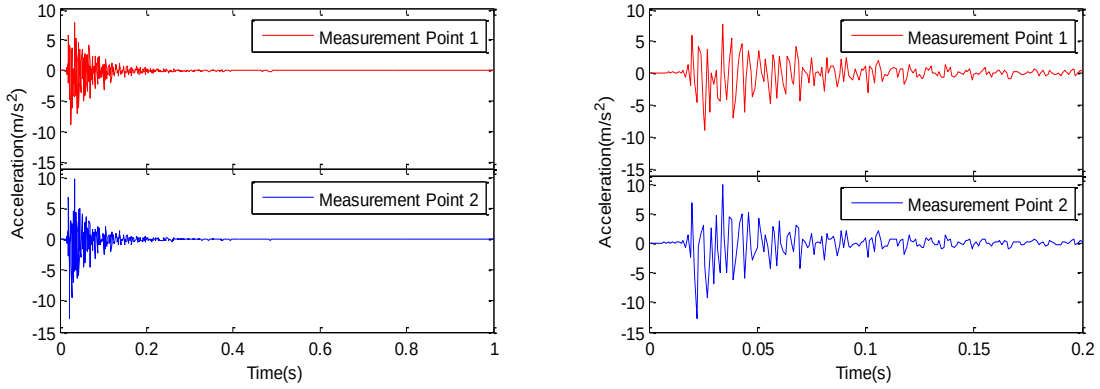

(a) Overview (b) Detailed plot

Fig. 2 Typical hit acceleration time histories of measurement points 1 and 2

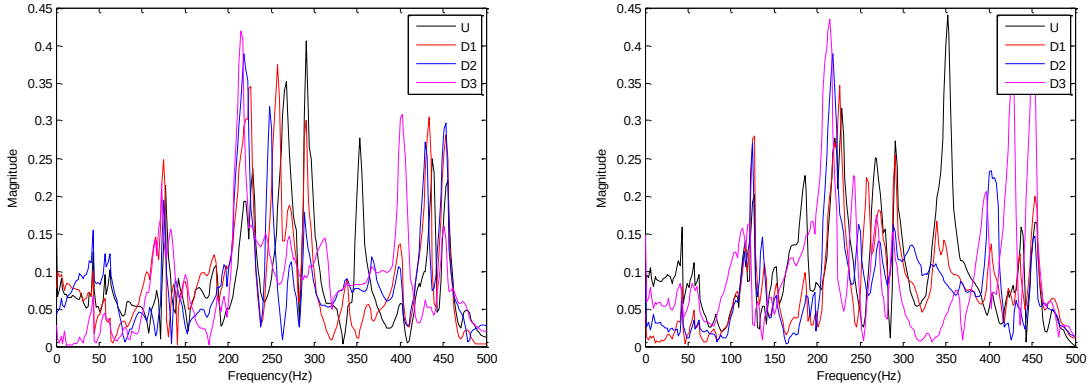

(a) Measurement point 1 (b) Measurement point 2

Fig. 3 Frequency responses under four conditions

The results of the bolt loosening detection are investigated to assess the feasibility of the statistical pattern recognition algorithm. As shown in Fig. 2(b), the hit acceleration time histories may be attenuated to a neglectable value within 0.2 s. Consequently, the first 0.2 s time histories of the measured structural response are used for damage detection. As the sampled frequency is 1000 Hz, the first 200-point measured time histories are used for the damage detection procedure. Each acceleration time history is divide into N = 50 individual data blocks, i.e., each data block includes L = 4 data points. The length of the root mean square acceleration would be 50, and the typical trend of the root mean square acceleration values for the hammer impact acceleration time history is depicted in Fig. 4. The normalized cross correlation function between root mean square acceleration of measurement points 1 and 2 is calculated by Eq. (4), and the typical normalized cross correlation function between root mean square acceleration of measurement points 1 and 2 is depicted in Fig. 5.

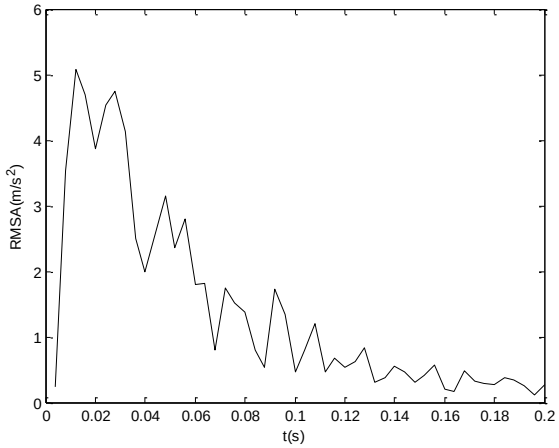

Fig. 4 Typical trend of the root mean square acceleration for the hammer impact acceleration time history

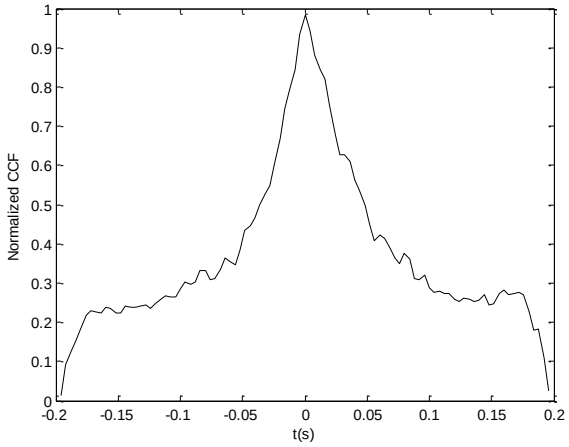

Fig. 5 Typical normalized cross correlation function between root mean square acceleration of measurement points 1 and 2

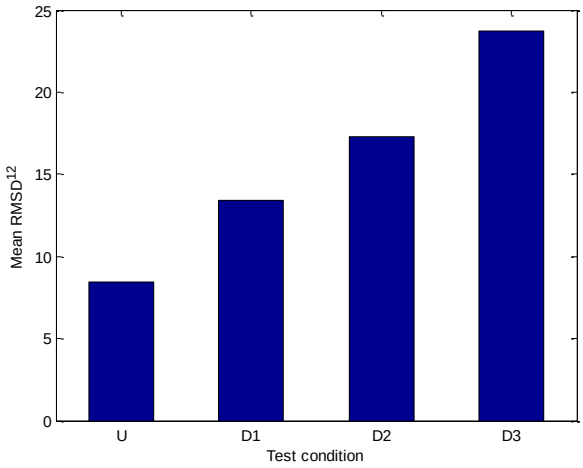

Fig. 6 The mean RMSD12 value of each test condition

Then the normalized cross correlation functions that derived from the healthy dataset are used for the calculation of RMSD[12], i.e., $\tilde{R}_{pq}^{D}(k)$ in Eq. (5) represents the normalized cross correlation function that derived from the healthy dataset. As there are 20 sets of time histories in the healthy dataset, 20 RMSD[12] samples can be extracted from the healthy dataset. Thereinafter, the normalized cross correlation functions that derived from each damage dataset are used for the calculation of RMSD[12], i.e., $\tilde{R}_{pq}^{D}(k)$ in Eq. (5) represents the normalized cross correlation function that derived from the damage dataset. 20 RMSD[12] samples can be extracted from each damage dataset.

The mean of the 20 RMSD[12] samples that extracted from the healthy dataset, and the mean of the 20 RMSD[12] samples that extracted from each damage dataset are calculated, with their results shown in Fig. 6. It is obvious that the mean RMSD[12] value grows regularly as the bolt loosening level increase. This demonstrates that the proposed feature RMSD is sensitive to bolt loosening that occurs in the tunnel lining, which validates the feasibility of RMSD in bolt loosening detection.

Finally, X-bar control chart is constructed by the 20 RMSD[12] samples that extracted from the healthy dataset. The control limits corresponding to a 99% confidence interval are constructed by setting α = 0.01 in Eq. (6). After the construction of control limits, the RMSD[12] samples obtained from each damage dataset are plotted along with the control limits, as shown in Fig. 7. The number of outliers are also summarized in Table 2, the percentages in the table represent the proportion of outliers in the total 20 RMSD[12] samples. For test condition U, there is no outlier, maybe because the bolt is not loosened. For test condition D1, there is also no outlier, maybe because the loosening of Bolt 23 under D1 does not have significant influence on the structure. For test condition D2, there are 50% samples outside the control limits. For test condition D3, all samples are outside the control limits. The percentage of outliers has an increasing tendency as the bolt loosening level increase.

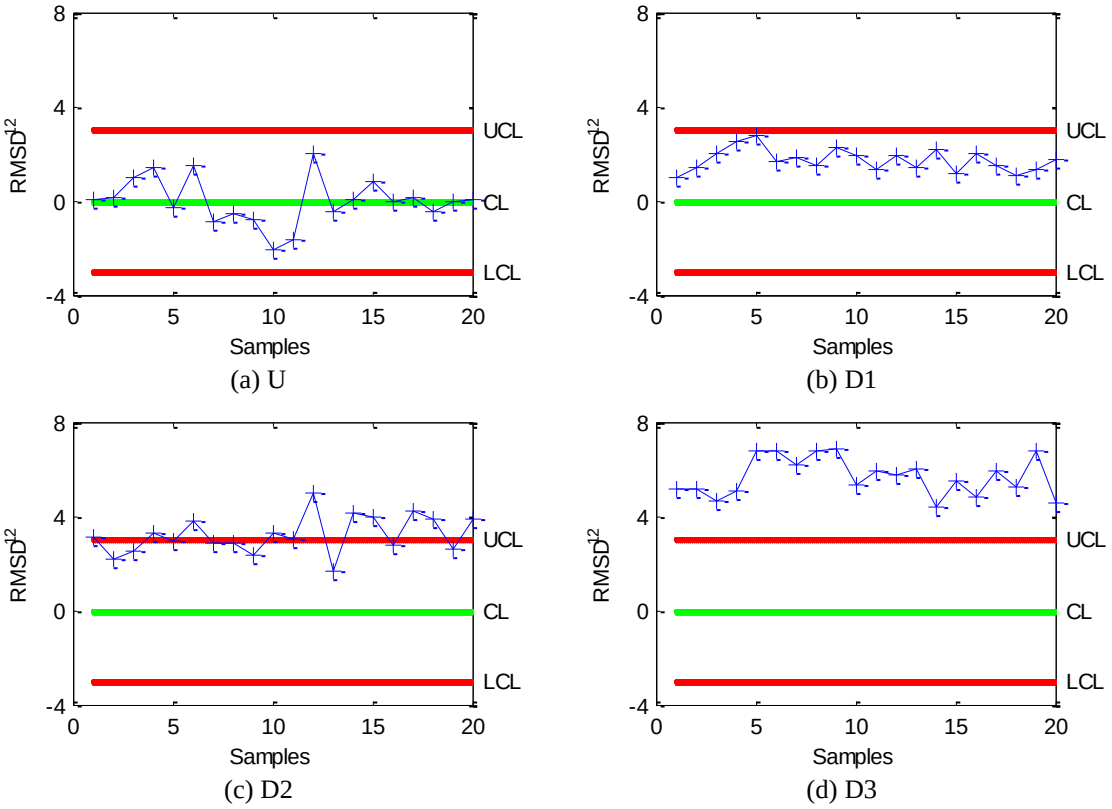

Fig. 7 X-bar control charts of the four test cases

Table 2 Outlier numbers of X-Bar control chart

	Condition			
	U	D1	D2	D3
Number of outliers	0	0	10	20
Percentages (%)	0	0	50	100

It is noted that the $RMSD^{12}$ values extracted from the healthy dataset are standardized prior to the construction of the X-bar control chart: the mean is subtracted from the features and the features is normalized by the standard deviation. Therefore, centerline for all figures in this paper corresponds to zero. The $RMSD^{12}$ values extracted from the damage dataset are also standardized in the same fashion as before. It is noted that the mean and standard deviation estimated from the healthy dataset are used to normalize the $RMSD^{12}$ values extracted from all the damage datasets.

7. Conclusions

This study proposes a root mean square acceleration and cross correlation function based method for the damage detection of subway tunnel lining. Root mean square deviations of the cross correlation functions before and after damage are chosen as damage sensitive features. Statistical process control charts are proposed to detect the variation of features before and after damage. A full-scale two-rings subway tunnel lining is constructed to validated the proposed algorithm, and damages are simulated by loosening the bolt that connecting adjacent segments. Results demonstrate that root mean square deviation is sensitive to bolt loosening, and the root mean square deviation value grows regularly as the bolt loosening level increase. In addition, the number of outliers in X-bar control chart increases with the increment of damage severity. The proposed data-based damage identification method is applicable to the online structural health monitoring system of subway tunnel lining, since the calculation of root mean square deviation and cross correlation function require low computational cost.

Acknowledgments

This work is supported by the grants from Basic Research Program of China (contract number: 2016YFC0802002), National Natural Science Foundation of China (NSFC, contract number: 51778258 and 51629801), the Research Funds from Wuhan Urban and Rural Construction Commission (Contract number: 201511, 201621, 201742), and the Fundamental Research Funds for the Central Universities (HUST: 2016JCTD113, 2014TS130 and 2015MS064).

References

Balsamo, L., Betti, R. and Beigi, H. (2014), "A structural health monitoring strategy using cepstral features", *J. Sound Vib*., **333**, 4526-4542.

Bennett, P.J., Soga, K., Wassell, I., Fidler, P., Abe, K., Kobayashi, Y. and Vanicek, M. (2010), "Wireless sensor networks for underground railway applications: case studies in Prague and London", *Smart Struct. Syst*., **6**(5-6), 619-639.

Carden, E.P. and Brownjohn, J.M.W. (2008), "ARMA modeled time-series classification for structural health monitoring of civil infrastructures", *Mech. Syst. Signal Pr*., **22**, 295-314.

Chen, B. and Xia, Y. (2017), "Advanced technologies in disaster prevention and mitigation", *Adv. Struct. Eng*., **20**(8), 1141-1142.

Chen, B., Weng, S., Zhi, L.H. and Li, D.M. (2017), "Response control of a large transmission-tower line system under seismic excitations by using friction dampers", *Adv. Struct. Eng*., **20**(8), 1155-1173.

Farrar, C.R. and Iii, G.H.J. (1997), "System identification from ambient vibration measurements on a bridge", *J. Sound Vib*., **205**(1), 1-18.

Farrar, C.R. and Worden, K. (2013), *Structural Health Monitoring: A Machine Learning Perspective*, John Wiley & Sons, Chichester, West Sussex, United Kingdom.

Farrar, C.R., Doebling, S. and Nix, D. (2001), "Vibration-based structural damage identification", *Philos. T. R. Soc. A*., **359**, 131-149.

Feng, L., Yi, X.H., Zhu, D.P., Xie, X.Y. and Wang, Y. (2015), "Damage detection of metro tunnel structure through transmissibility function and cross correlation analysis using local excitation and measurement", *Mech. Syst. Signal Pr*., **60-61**, 59-74.

Li, P.Y., Chen, B., Xie, W.P and Xiao, X. (2015), "A comparative study on frequency sensitivity of a

transmission tower", *J. Sensors*, **2015**(2), 1-14.
Mosavi, A.A., Dickey, D., Seracino, R. and Rizkalla, S. (2012), "Identifying damage locations under ambient vibrations utilizing vector autoregressive models and mahalanobis distances", *Mech. Syst. Signal Pr.*, **26**, 254-267.
Noman, A.S., Deeba, F. and Bagchi, A. (2013), "Health monitoring of structures using statistical pattern recognition techniques", *J. Perform. Constr. Fac.*, **27**(5), 575-584.
Pandit, S.M. and Wu, S.M. (1983), *Time Series and System Analysis with Applications*, John Wiley & Sons, New York, NY, USA.
Richards, J.A. (1998), "Inspection, maintenance and repair of tunnels: international lessons and practice", *Tunn. Undergr. Sp. Tech.*, **13**(4), 369-375.
Rzeszucinski, P.J., Sinha, J.K., Edwards, R., Starr, A. and Allen, B. (2012), "Normalised root mean square and amplitude of sidebands of vibration response as tools for gearbox diagnosis", *Strain*, **48**(6), 445-452.
Sekine, M., Tamura, T., Yoshida, M., Suda, Y., Kimura, Y., Miyoshi, H. Kijima, Y., Higashi, Y. and Fujimoto, T. (2013), "A gait abnormality measure based on root mean square of trunk acceleration", *J. Neuroeng. Rehabil.*, **10**(1), 1-7.
Sohn, H. and Farrar, C.R. (2001), "Damage diagnosis using time series analysis of vibration signals", *Smart Mater. Struct.*, **10**(3), 446-451.
Sohn, H., Czarnecki, J.A. and Farrar, C.R. (2000), "Structural health monitoring using statistical process control", *J. Struct. Eng.*, **126**(11), 1356-1363.
Vecer, P., Kreidl, M. and Smid, R. (2005), "Condition indicators for gearbox condition monitoring systems", *Acta Polytech.*, **45**(6), 35-43.
Xiao, H.T., Lou, S. and Ogai, H. (2015), "A novel bridge structure damage diagnosis algorithm based on post-nonlinear ICA and statistical pattern recognition", *IEEJ T. Electr. Electr.*, **10**(3), 287-300.
Yi, T.H., Li, H.N. and Gu, M. (2011), "Optimal sensor placement for structural health monitoring based on multiple optimization strategies", *Struct. Des. Tall Spec.*, **20**(7), 881-900.
Yi, T.H., Li, H.N. and Gu, M. (2013), "Recent research and applications of GPS-based monitoring technology for high-rise structures", *Struct. Control Health.*, **20**(5), 649-670.
Zhou, B., Xie, X.Y., Yang, Y.B. and Jiang, J.C. (2012), "A novel vibration-based structure health monitoring approach for the shallow buried tunnel", *CMES-Comp. Model. Eng.*, **86**(4), 321-348.
Zhu, D.P., Yi, X.H., Wang, Y. and Sabra, K. (2010), "Structural damage detection through cross correlation analysis of mobile sensing data", *Proceedings of the 5th World Conference on Structural Control and Monitoring*, Tokyo, Japan, July.
Zhu, H.P., Luo, H., Ai, D.M. and Wang, C. (2016), "Mechanical impedance-based technique for steel structural corrosion damage detection", *Measurement*, **88**, 353-359.

TY